Supplementary Information

for

Engineering of Thermo-/pH-Responsive Membranes with Enhanced Gating Coefficients, Reversible Behavior and Self-Cleaning Performance through Acetic Acid Boosting Microgels Assembly

Huawen Liu [a, †], Xueting Zhao [a, †], Ning Jia [a], Arcadio Sotto [b], Yan Zhao [c], Jiangnan Shen [a, *], Congjie Gao [a] and Bart van der Bruggen [c]

[a] *Center for Membrane Separation and Water Science & Technology, Ocean College, Zhejiang University of Technology, Hangzhou 310014, China*

[b] *School of Experimental Science and Technology, ESCET, Rey Juan Carlos University, E-28933 Móstoles, Madrid, Spain*

[c] *Department of Chemical Engineering, KU Leuven, Celestijnenlaan 200F, B-3001 Leuven, Belgium*

[*] *Corresponding author: J. Shen (shenjn@zjut.edu.cn).*

[†] *Contributed equally to this work.*

Note S1. Synthesis of Poly(NIPAM-co-MAA) Microgels

The poly (NIPAM-co-MAA) nanoparticles were synthesized by free-radical copolymerization in the aqueous solution. For example, 28 mmol sample of comonomer in different NIPAM/MAA ratios, 5.0 mol% (of total monomer) MBA and 0.04 mmol of SDS were dissolved in 400 mL of deoxygenated water in a 500 mL of three-necked flask. Under a nitrogen atmosphere, the resultant solution was heated to 75 °C. Then, 1.0 mol % (of total monomer) APS dissolved in 2 mL of water was added to start the reaction. The solution became turbid after 20 min, indicating that the particles have formed. These particles were left to polymerize for a further 3 h. The P(NIPAM-co-MAA) microgels were purified to remove the residual and unreacted components by more than 5 times centrifugation/redispersion cycles. The speed of centrifugation is 10000 rpm. The purified P(NIPAM-co-MAA) microgels were freeze-dried at - 49 °C for 48 h and reserved for further use. In this work, the feed molar ratios of MAA to NIPAM are 1:9, 2:8, 3:7 and 5:5, and accordingly the microgels are noted as N0.1, N0.2, N0.3 and N0.5, respectively. The yield of N0.1, N0.2, N0.3 and N0.5 were 61.95%, 64.13%, 73.45%, 72.24%, respectively.

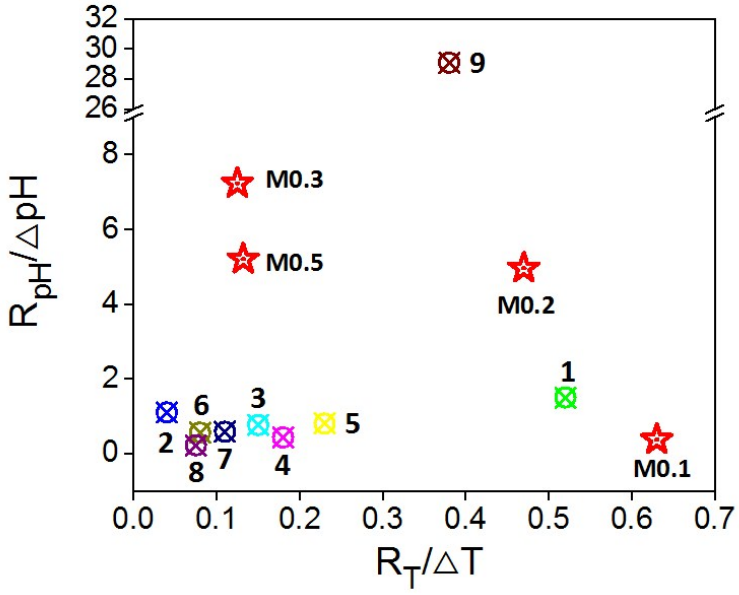

Fig. S1. The unitary gating ratios ($R_T/\triangle T$ and $R_{pH}/\triangle pH$) of dual thermo- and pH- responsive membrane that have been reported and worked in this study. The red pentagrams represent the performance of the DRMs in this work. The $R_T/\triangle T$ of membranes M0.1, M0.2, M0.3 and M0.5 in this work were taken from 30°C to 40°C at pH 3, and the $R_{pH}/\Delta pH$ in this work was taken from pH 3 to pH 9 at 45 °C. The unitary gating ratios are taken from one of the most optimized membranes in each literature.[1-9] The numbers in the figure are correspond to the numbers of the references. The calculated range of temperature and pH is taken from around the turning point of the water gating.

Fig. S1 shows the gating ratio of dual thermo- and pH- responsive membrane in this work and references. The unitary thermo-responsive gating ratio ($R_T/\triangle T$) and the unitary pH-responsive gating ratio ($R_{pH}/\triangle pH$) was determined by the unitary ratio of trans-membrane water fluxes and calculated by the following equations:

$$R_T \Big/ \Delta T = \frac{J_s(b°C)/J_s(a°C)}{b - a} \quad (1)$$

$$R_{pH} \Big/ \Delta pH = \frac{J_s(pH\ d)/J_s(pH\ c)}{d - c} \quad (2)$$

where *Js (b°C)* (kg m^{-2} h^{-1}) is the water flux tested at b °C when the gates open; *Js (a°C)* is the water flux tested at a °C when the gates close; *Js (pH d)* is the water flux tested at *pH d* when the gates open; *Js (pH c)* is the water flux tested at *pH c* when the gates close.

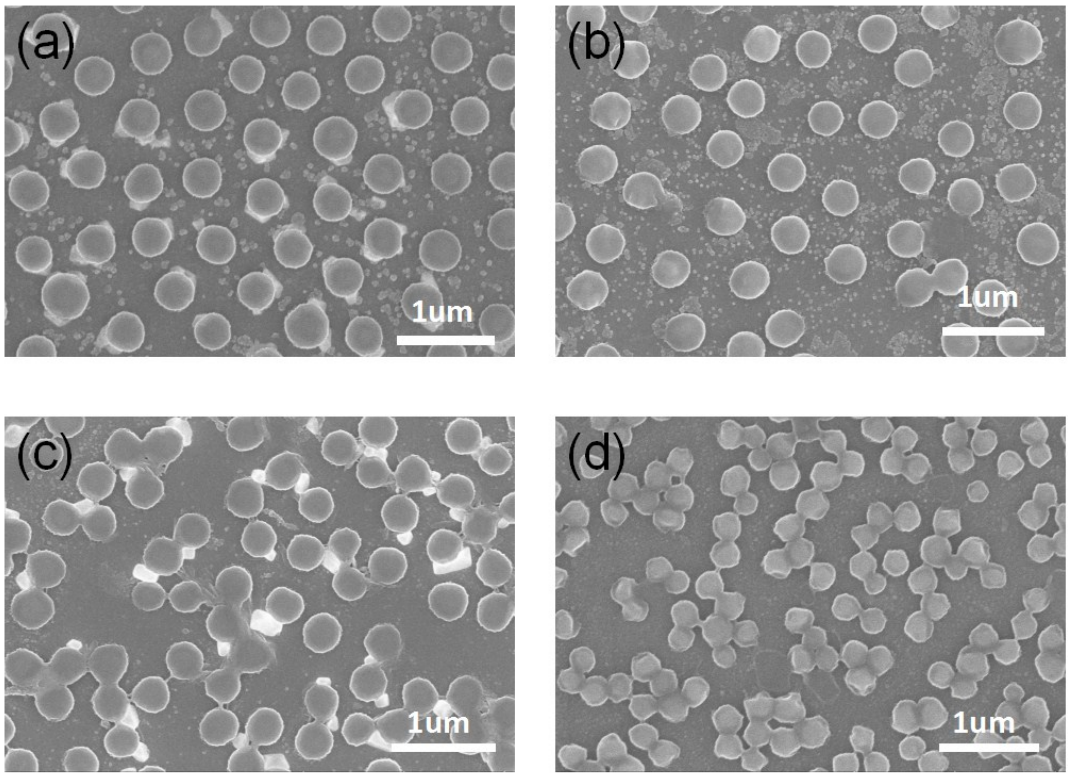

Fig. S2. SEM images of microgels. (a), (b), (c) and (d) SEM of N0.1, N0.2, N0.3 and N0.5 microgels respectively.

The scanning electron microscope (SEM) images of microgels are displayed in Fig. S2. This confirms that the microgels are shown good monodispersity, spherical shape and uniform size. The size of dried microgel N0.1, N0.2, N0.3, N0.5 is 400±22 nm, 390±20 nm, 370±25 nm and 250±20 nm, respectively.

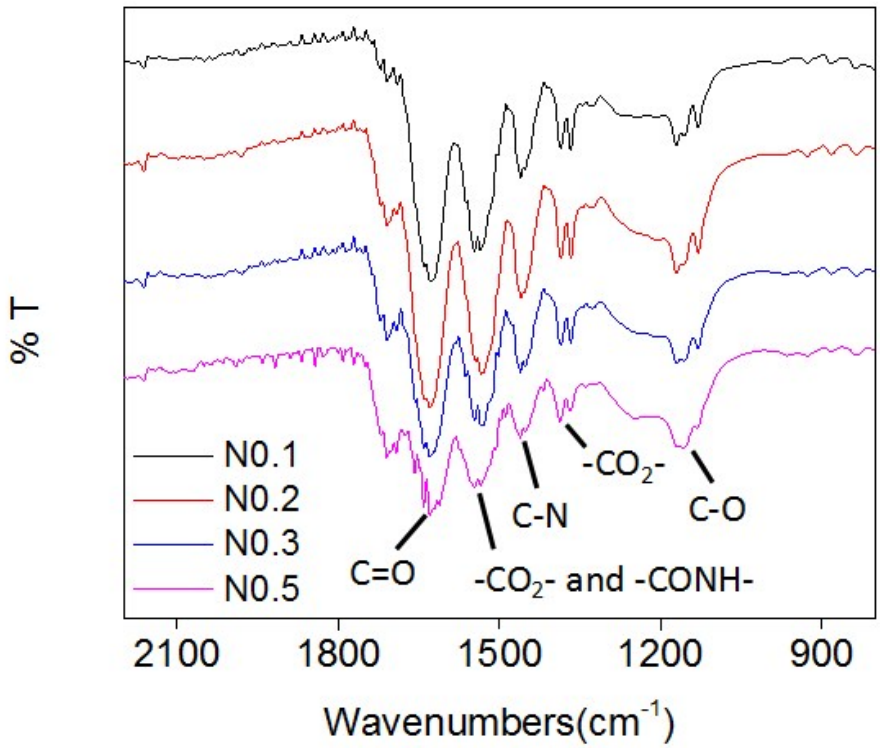

Fig. S3. FTIR spectrum of microgels.

The state of microgels was studied by fourier-transform infrared (FTIR) spectroscopy. As shown in Fig. S3, absorption bands at around 1620 cm^{-1} is attributed to the stretching vibration of C=O of NIPAM and MAA. The absorption bands at around 1540 cm^{-1} is assigned to the stretching vibrations of amide group and carboxylic groups. The absorption bands at around 1450 cm^{-1} is assigned to the stretching vibration of C-N of NIPAM. The absorption bands at 1400 cm^{-1} is attributed to the symmetrical stretching vibration of carboxylic groups. The absorption bands at around 1180 cm^{-1} is assigned to the stretching vibrations of C-O of carboxylic groups. This confirms that the microgels have NIPAM group and MAA group.

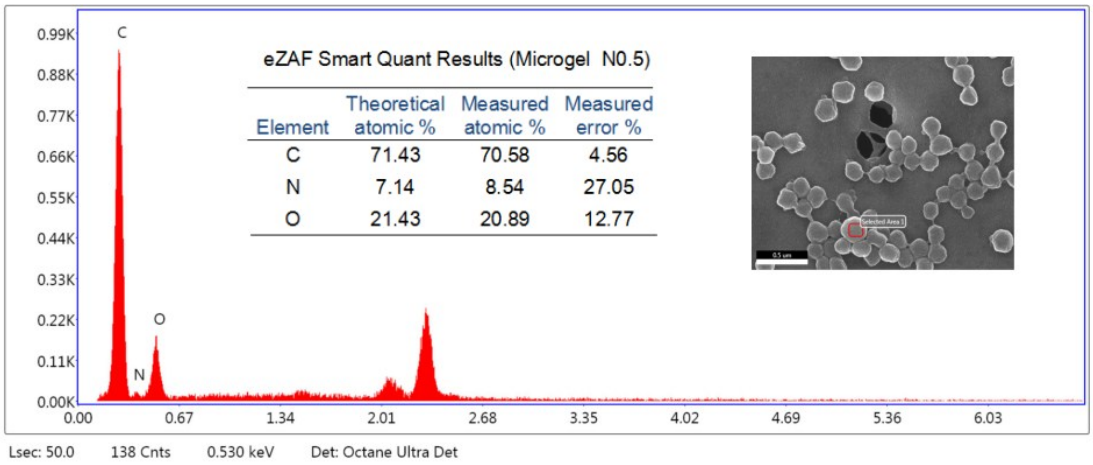

Fig. S4. The EDS of microgel N0.5.

The energy dispersive spectrometer (EDS) performed on these samples suggests that three elements C, N and O are in the microgel N0.5 sample with 70.58:8.54:20.89 atomic ratio. The measured atomic ratios are similar to the theoretical atomic ratios (the molar ratios of MAA to NIPAM is 5:5).

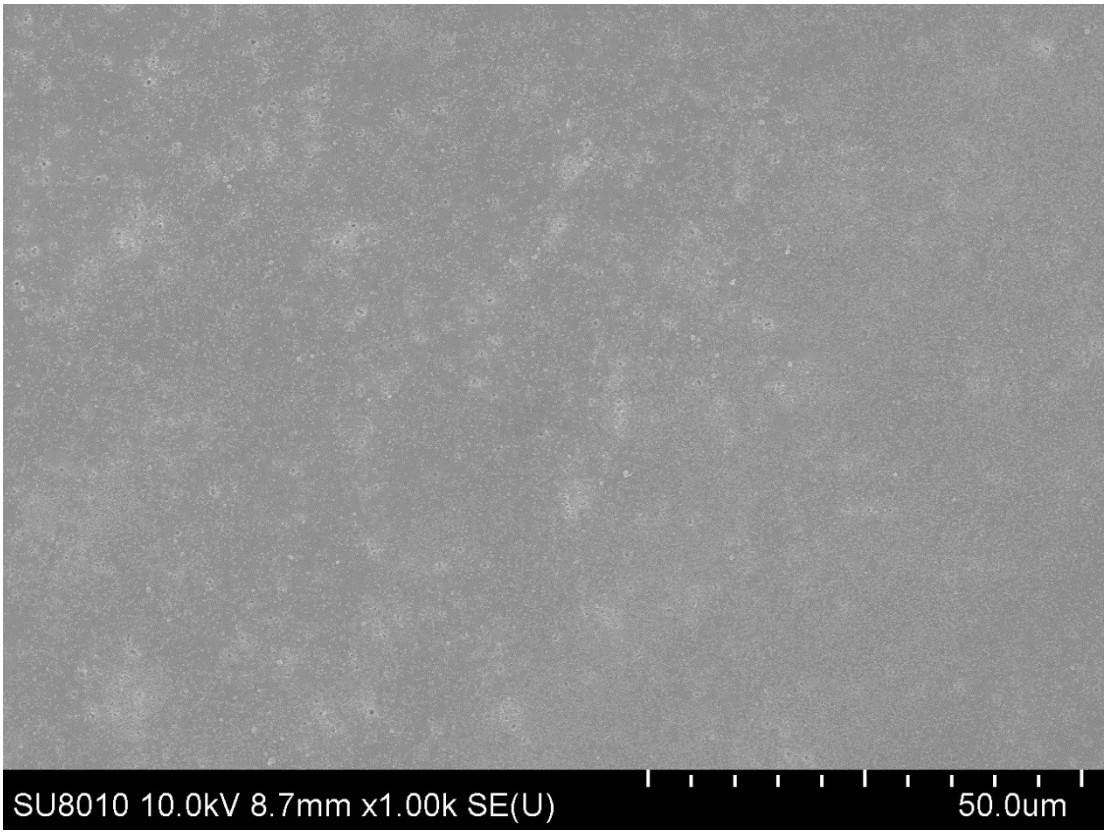

Fig. S5. SEM image of surface view of membrane M0.3.

The SEM image of membrane M0.3 is presented in Fig. S5. This confirms that the microgels are uniformly distributed on the surface of the membrane.

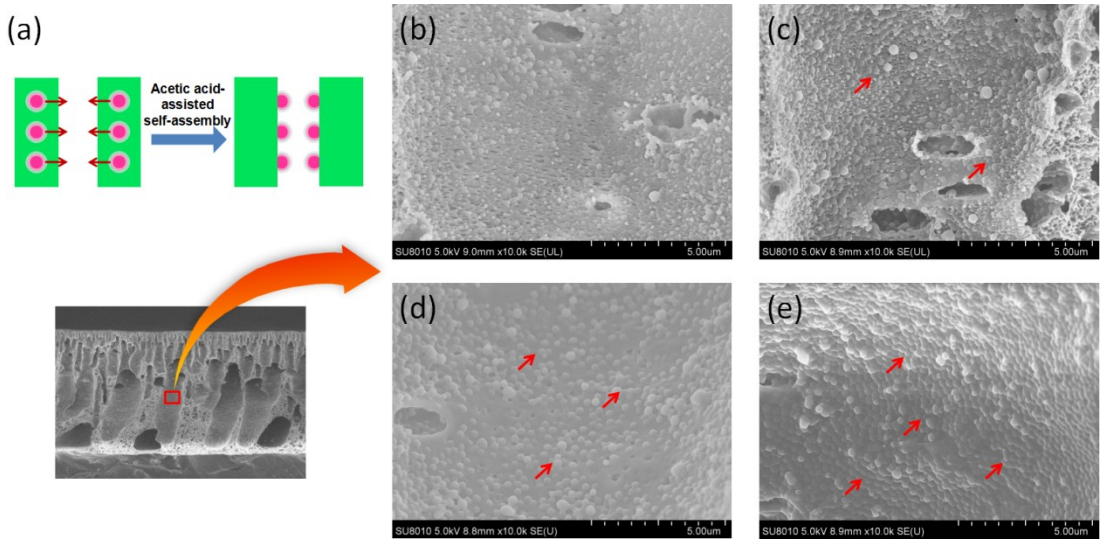

Fig. S6. (a) Schematic illustration of the self-assembly procedure of microgels through an acetic acid-assisted method. (b), (c), (d) and (e) SEM images of magnified cross-sections of membranes assisted by 0%, 7.5%, 15% and 30% volume fraction of acetic acid in water respectively.

From Fig. S6b to Fig. S6e, the number of microgels assembled on the channel surface was gradually increasing with the increasing ratio of acetic acid in water. While the volume fraction of acetic acid in water is more than 15%, a large number of microgels are distributed on the surface of channels. This shows that acetic acid have a great contribution on the segregation of microgels.

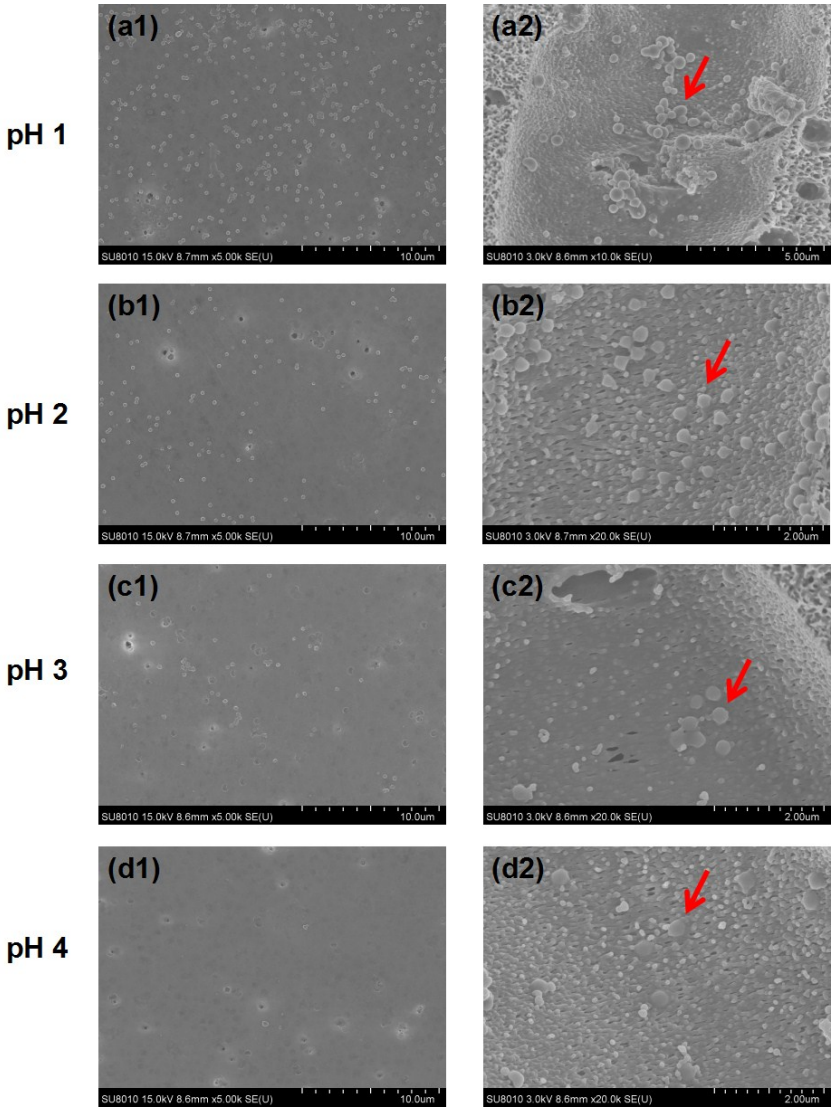

Fig. S7. SEM images of surfaces (a1-d1) and magnified cross-sections (a2-d2) of membranes prepared with different pH coagulation bath. The coagulation bath was adjusted by hydrochloric acid.

Fig. S7 shows that there were some microgels distributed on the membrane surface. However, The microgels were failed to segregate on the surface channels. This indicates that the coagulation bath with low pH value have a tiny contribution on microgels segregation and the segregation ability of acetic acid cannot be replaced by hydrochloric acid during the coagulation step of the phase-inversion process.

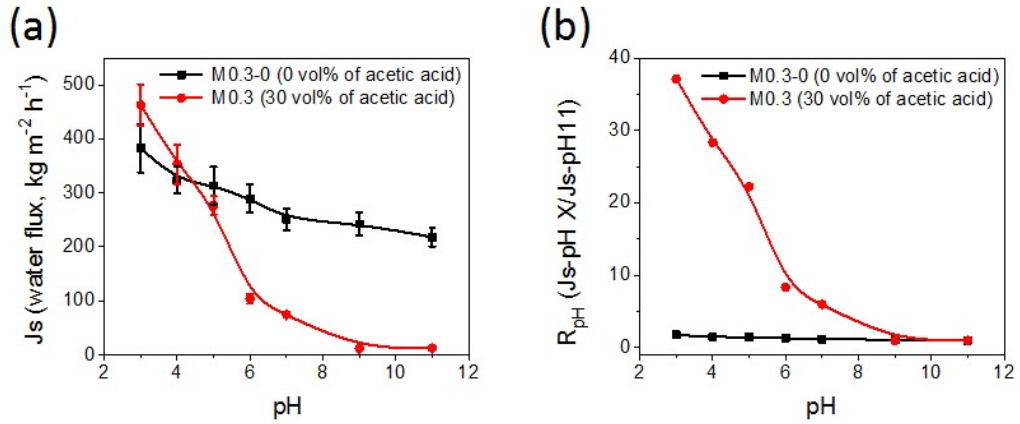

Fig. S8. (a) The water fluxes of membranes at different pH. The membrane M0.3-0 and M0.3 was prepared by the coagulation bath with 0 vol% and 30 vol% of acetic acid in water, respectively. (b) The pH-responsive gating coefficients (R_{pH}) of membranes. The R_{pH} is defined as the ratio of trans-membrane water fluxes at pH x to that at pH 11.

As shown in Fig. S8, The water fluxes of the membrane M0.3-0 varies from 383 kg m^{-2} h^{-1} (pH 3) to 218 kg m^{-2} h^{-1} (pH 11) with a gating coefficient of about 1.8. The water fluxes of optimized membrane M0.3 varies from 463 kg m^{-2} h^{-1} (pH 3) to 12.5 kg m^{-2} h^{-1} (pH 11) with a gating coefficient of 37. This shows that the optimum smart gating membrane with *in situ* assembled microgels as gates can enhance the gating coefficients.

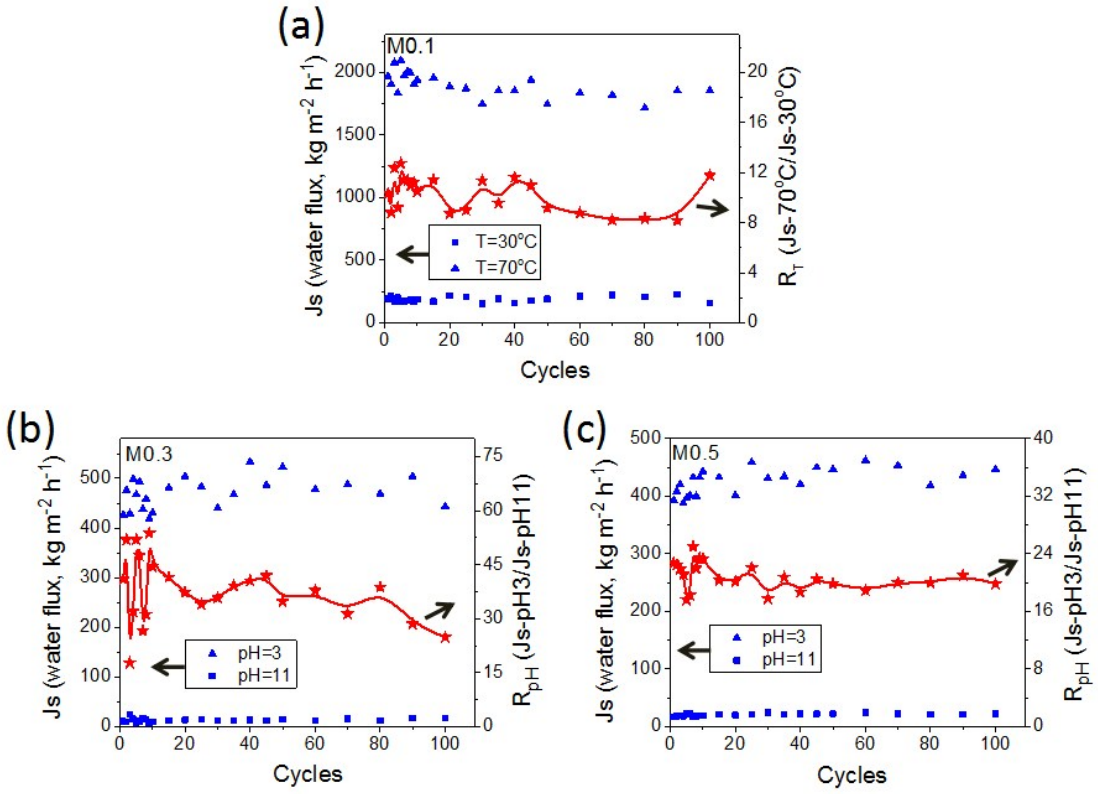

Fig. S9. (a) The thermo-reversible water fluxes and gating coefficients (R_T) of membrane M0.1 at 30°C/pH 3 or 70 °C/pH 3. (b) and (c) The pH-reversible water fluxes and gating coefficients (R_{pH}) of membrane M0.3 and membrane M0.5 at pH 3/30 °C or pH 11/30 °C, respectively.

As shown in Fig. S9, the membrane M0.1 had excellent thermo-reversible performance, and the membrance M0.3 and M0.5 both had excellent pH-reversible performance.

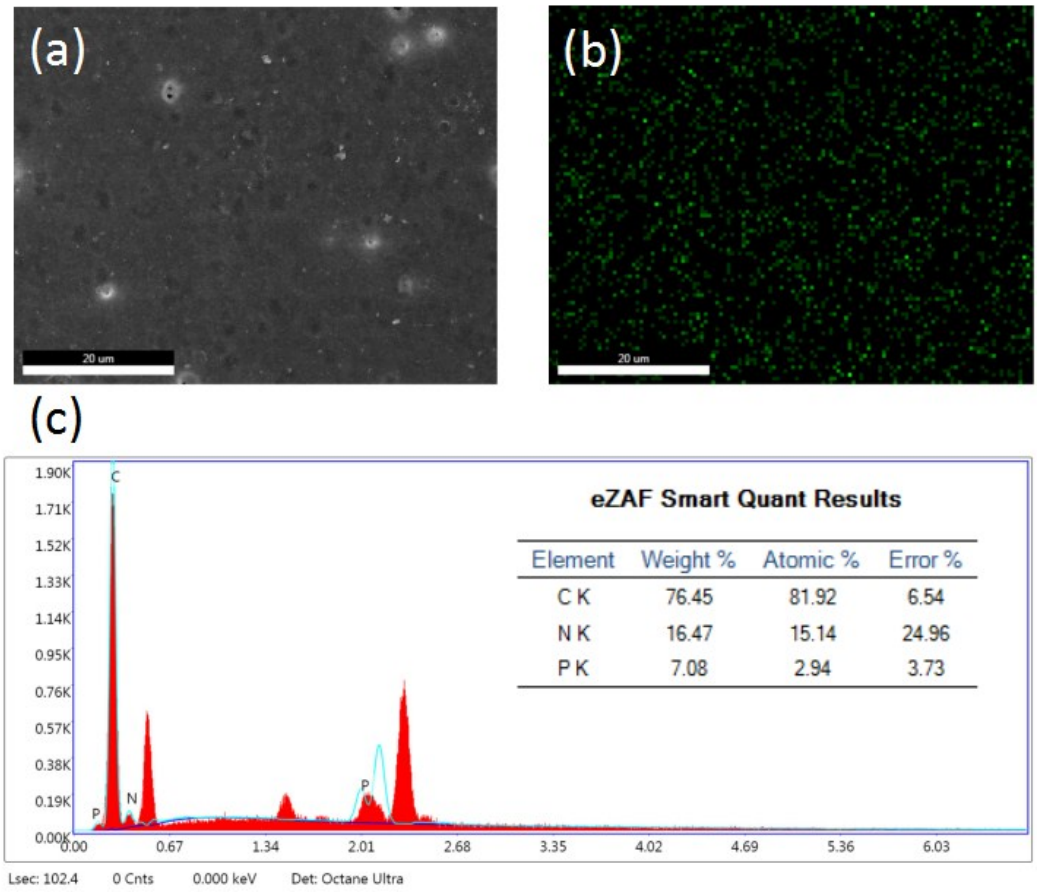

Fig. S10. (a) SEM of membrane M0.3 contaminated by BSA. (b) EDS maps of BSA-contaminated M0.3. (c) EDS of BSA-contaminated M0.3.

The scanning electron microscope (SEM) image of contaminated M0.3 is displayed in Fig. S10a. The energy dispersive spectrometer (EDS) is shown in Fig. S10c, indicating that phosphorus elements are distributed on surface of membrane. The EDS maps shows that phosphorus elements are evenly distributed on membrane surface (Fig. S10b). This is suggests that the membrane M0.3 was polluted by bovine serum albumin (BSA).

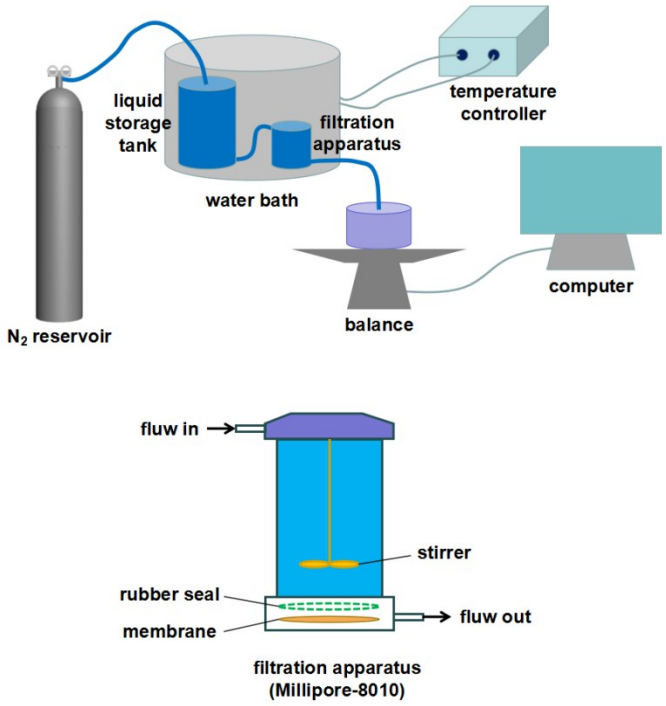

Fig. S11. Schematic of water flux measurement device (up) and a filtration apparatus (down).

The water fluxes were carried out with a "dead-end" filtration apparatus (Millipore-8010) with the cell volume of 10 mL and the effective area of 3.464 cm^{-2}. The membrane was placed at the bottom of the filtration cell, and tightly sealed by rubber seal to prevent solution leakage. The temperature of permeate liquid was controlled with a temperature-controller, while pH was adjusted by addition of hydrochloric acid and sodium hydroxide solution. The permeate liquid was stirred at a speed of 100 rpm by the stirrer. The trans-membrane pressure was provided by nitrogen gas pressure. The entire filtration apparatus and the feed system were soaked in the water bath to obtain the measured temperature.

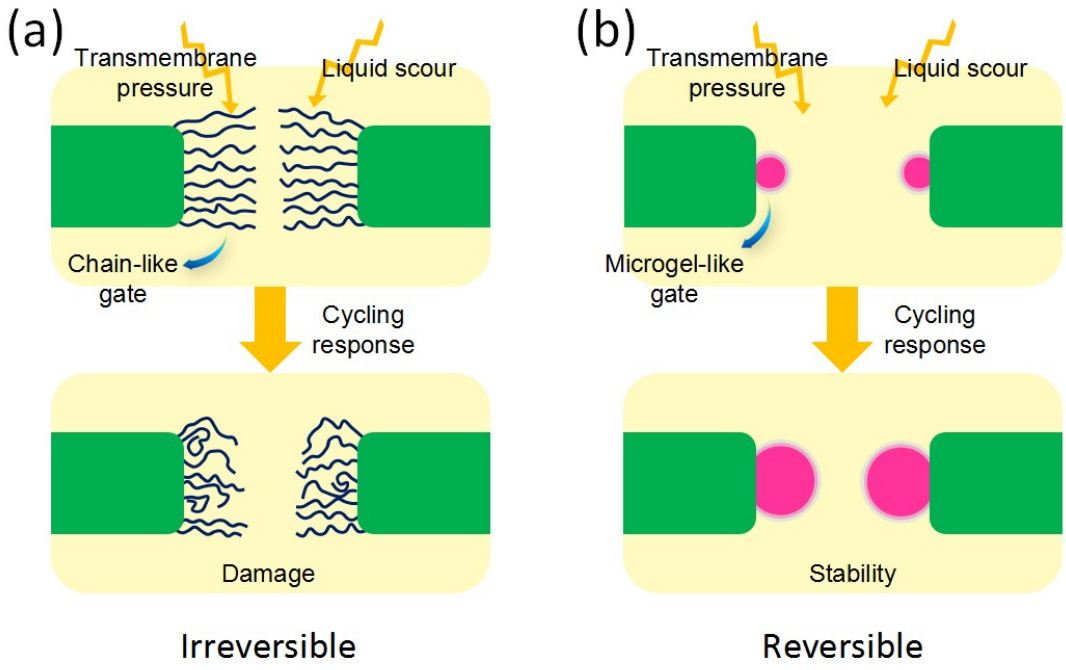

Fig. S12. Schematic of (a) the damage of chain-like gate and (b) the stability and reversibility of structurally stable microgel-like gate under the transmembrane pressure and scouring of liquid.

References

1. K. Pan, X. Zhang, R. Ren and B. Cao, *Journal of Membrane Science*, 2010, **356**, 133-137.
2. Y. M. Lee and J. K. Shim, *Polymer*, 1997, **38**, 1227-1232.
3. Z. B. Zhang, X. L. Zhu, F. J. Xu, K. G. Neoh and E. T. Kang, *Journal of Membrane Science*, 2009, **342**, 300-306.
4. K. Pan, R. Ren, H. Li and B. Cao, *Polymers for Advanced Technologies*, 2013, **24**, 22-27.
5. Y.-C. Chen, R. Xie and L.-Y. Chu, *Journal of Membrane Science*, 2013, **442**, 206-215.
6. F. Schacher, M. Ulbricht and A. H. E. Müller, *Advanced Functional Materials*, 2009, **19**, 1040-1045.
7. J. Xue, L. Chen, H. L. Wang, Z. B. Zhang, X. L. Zhu, E. T. Kang and K. G. Neoh, *Langmuir : the ACS journal of surfaces and colloids*, 2008, **24**, 14151-14158.
8. Z. Yi, L.-P. Zhu, Y.-Y. Xu, X.-L. Li, J.-Z. Yu and B.-K. Zhu, *Journal of Membrane Science*, 2010, **364**, 34-42.
9. B. Ma, X.-J. Ju, F. Luo, Y.-Q. Liu, Y. Wang, Z. Liu, W. Wang, R. Xie and L.-Y. Chu, *ACS applied materials & interfaces*, 2017, **9**, 14409-14421.